2-Axis Magnetometers Based on Full Wheatstone Bridges Incorporating Magnetic Tunnel Junctions Connected in Series

Ricardo Ferreira[1], Elvira Paz[1], Paulo P. Freitas[1,2,4], João Ribeiro[3,4], José Germano[3], and Leonel Sousa[3,4]

[1]INL-International Iberian Nanotechnology Laboratory, 4715-330 Braga, Portugal
[2]INESC-MN/Institute for Nanosciences and Nanotechnologies, 1000-029 Lisbon, Portugal
[4]IST-Instituto Superior Técnico, Universidade Técnica de Lisboa, 1049-001 Lisbon, Portugal
[3]INESC-ID, 1000-029 Lisbon, Portugal

Full Wheatstone Bridge incorporating a serially connected ensemble of Magnetic tunnel junctions was produced, targeting an application as a magnetic field compass. To that end, MTJs with $\mathrm{RxA} \sim 10\ \mathrm{k\Omega}\ \mu\mathrm{m}^2$, $\mathrm{TMR} \sim 150$–200%, $\mathrm{Hf} = 5\ \mathrm{Oe}$ and $\mathrm{Hf} = 5\ \mathrm{Oe}$ were produced. In order to achieve a full bridge signal, two stacks with an asymmetric SAF reference structure where used to produce MTJs with opposite dR/dH upon annealing in the same substrate. The resulting Bridges exhibit sensitivities between 13.5–32 mV/V/Oe depending on the field range and provide a significantly advantageous alternative to AMR and GMR based bridges.

***Index Terms*—Magnetic field sensors, magnetic tunnel junctions, magnetometers, wheatstone bridges.**

I. Introduction

MAGNETORESISTIVE Sensors are becoming increasingly important in large industrial domains such as the automotive industry. Magnetic field sensors based on the anisotropic magnetoresistance (AMR) or giant magnetoresistance (GMR) effects are nowadays commonly used as angular displacement or electrical current monitoring sensors. For such practical applications, the stability of the sensor output must be ensured over a large range of temperatures. This demand is usually met by integrating the sensors in Full Wheatstone Bridges which also provides a null-voltage output in the absence of an external stimulation field, while ensuring the same full output voltage of a single device [1].

The replacement of spin valves (SV) and AMR sensors by Magnetic tunnel junctions (MTJ) should result in devices with enhanced magnetic field sensitivity taking profit of the very large tunneling magnetoresistance (TMR) effect which can be as large as 600% [2] in the CoFeB/MgO/CoFeB system. Full MTJ bridges have already been produced for applications with integrated magnetic field sources [3]. However, for applications with an external field source, the integration of CoFeB/MgO/CoFeB magnetic tunnel junctions in full bridges is not straightforward: the setting of the two different and symmetric orientations required for the magnetization of the pinned layer in adjacent arms of the bridge (Fig. 1) is not easily achieved due to the simultaneous requirement of high annealing temperature to crystallize the CoFeB ($\sim 330^{\circ}\mathrm{C}$) and reach high TMR values. Furthermore, a good linear response in CoFeB/MgO/CoFeB usually relies in the use of thin CoFeB layers [4] associated with an out-of-plane magnetization component [5] or superparamagnetic behavior [6], [7] which also result in a decreased TMR effect due to the reduced electrode thickness [8], [9]. A local current-assisted annealing to selectively rotate the pinned layer of two linear MTJs (with thin CoFeB) in a bridge upon microfabrication was already demonstrated [10]. While this method is successful, it cannot be applied at a production scale (each individual device must be electrically contacted) and the large currents across the thin tunnel barriers deteriorate the MTJ response with a detrimental effect over the reproducibility and reliability of the method.

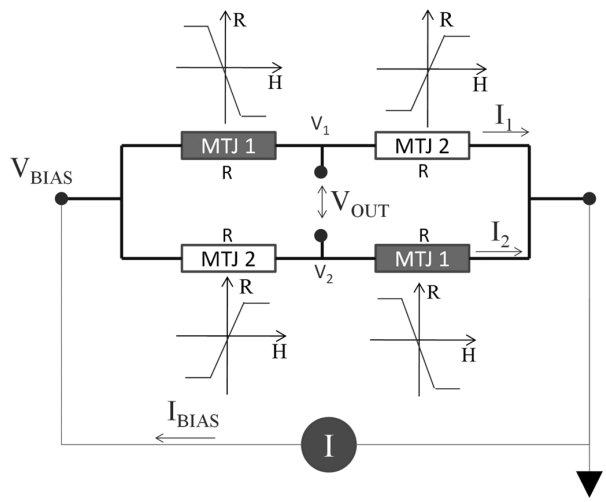

Fig. 1. Full Wheatstone Bridge incorporating magnetoresistive devices. In order to achieve a full bridge output two types of devices with opposite dR/dH are required.

This work demonstrates a method to produce Full Wheatstone Bridges incorporating full signal linear MTJs connected in series ($\mathrm{TMR} = 150$–200%). These bridges were used to manufacture a 2-axis magnetometer which was then incorporated in a digital compass electronic platform and successfully used to detect the orientation of the digital compass with respect to the earth's magnetic field.

II. Sample Preparation

In order to obtain the full bridge magnetometer, MTJs where produced starting from stacks of type $\mathrm{Buffer/7.5Ir_{20}Mn_{80}/2.0Co_{70}Fe_{30}/0.85Ru/2.6Co_{40}Fe_{40}B_{20}/MgO/3.0Co_{40}Fe_{40}B_{20}/0.21Ta/16Ni_{81}Fe_{19}/Cap}$ [nm]

Manuscript received March 02, 2012; revised April 27, 2012 and May 14, 2012; accepted May 25, 2012. Date of current version October 19, 2012. Corresponding author: R. Ferreira (e-mail: ricardo.ferreira@inl.int).

Digital Object Identifier 10.1109/TMAG.2012.2202381

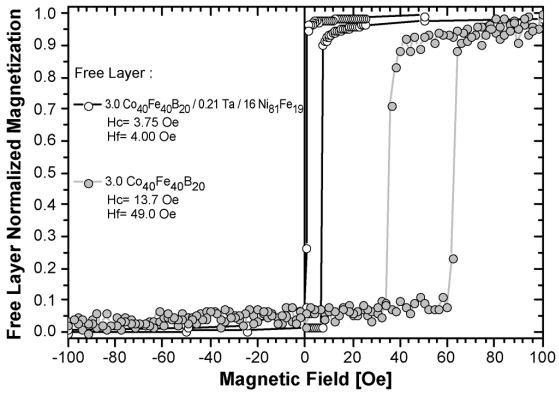

Fig. 2. VSM Plot of two MTJs of Type 1, incorporating two different free layers. The introduction of a thick NiFe layer singnificantly reduces $\mathrm{H_c}$ and $\mathrm{H_f}$. CIPT measurements indicate that TMR remains unaffected at 200% in both types of stacks.

(Type 1). A modified stack with an additional layer coupled in the reference SAF was then deposited in the same wafer. This second stack was of the type $\mathrm{Buffer/7.5Ir_{20}Mn_{80}/2.0Co_{70}Fe_{30}/0.85Ru/2.0Co_{70}Fe_{30}/0.85Ru/2.6Co_{40}Fe_{40}B_{20}/MgO/3.0Co_{40}Fe_{40}B_{20}/0.21Ta/16Ni_{81}Fe_{19}/Cap\ [nm]}$ (Type 2). The MTJ stacks were deposited in a TIMARIS PVD system with a base pressure of 2.0×10^{-9} mbar.

The MgO barrier of the MTJ stacks was formed starting from a ceramic target and the thickness of the layer was chosen targeting a RxA value in the range of 10 $\mathrm{k\Omega\mu m^2}$.

The sensing layer structure was optimized in order to provide devices with low coupling field $(\mathrm{H_f})$ and low coercive field $(\mathrm{H_c})$ while still maintaining the large TMR characteristic of CoFeB/MgO/CoFeB MTJs. To that end, a thin 0.21 nm Ta dusting layer was inserted between the CoFeB and NiFe layers in the top free layer. This Ta layer is thin enough to ensure that CoFeB and NiFe remain ferromagnetically coupled and thick enough to prevent the crystalline structure of the NiFe to propagate to the CoFeB layer during annealing, thus preserving the proper CoFeB bcc 100 texture and high TMR which would be lost without it. Current-in-plane Tunneling Magnetoresistance (CIPT) measurements of the unpatterned stacks shown in Fig. 2 (with and without Ta/NiFe in the sensing layer) indicate that the TMR remains at 180–200% with the NiFe introduction. The introduction of NiFe in the free layer, in the first place, is required in order to achieve high bridge sensitivities. In order to linearize the MTJ output (using the device shape anisotropy) and overlap the linear range of both types of MTJs in the bridge the demagnetizing field must become dominant over both the coercive field $(\mathrm{H_c})$ and ferromagnetic coupling field $(\mathrm{H_{f.}})$. As shown in Fig. 2, in stacks without NiFe, the switching fields in the unpatterned stacks are as large as 60 Oe. With the introduction of NiFe the switching fields in can be reduced to under 10 Oe which should allow the production of linear MTJs with linear ranges of the order of 20 Oe using shape anisotropy alone.

In order to deposit the two types of MTJ stacks on the same wafer, each of the MTJs stacks is selectively deposited on a selected region of the wafer surface using a lift-off step. At this point, the wafer with both stacks is then annealed at 330°C for 2 hours under a magnetic field of 1 T. Each of these stacks

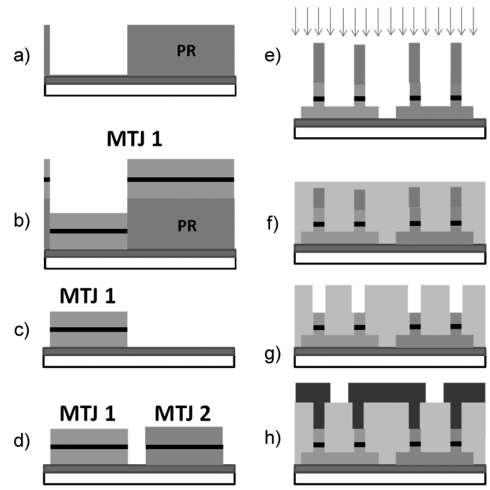

Fig. 3. Microfabrication process flow used to manufacture the full Wheatstone Bridges. A photo-resist mask is defined to delimit the area of the wafer which will be occupied by MTJs of type 1 (a). The MTJ stack type 1 is deposited (b) and a lift-off process is used to delimit the stack (c) onto the region which will form the bridge branches with type 1 MTJs. This process is repeated in order to define the regions making the bridge branches with type 2 MTJs (d). Once both types of MTJs are present in the same wafer an annealing step is performed in order to set the exchange. A self-aligned microfabrication process is then carried on to terminate the device. A mask is deposited to define the MTJ pillars which are defined by Ion Milling and an insulation oxide is deposited without removing the photo-resist (f). Via opening through the insulation oxide is made via lift-off (g) and metal contacts are finally fabricated by lift-off defining the Wheatstone bridge (h).

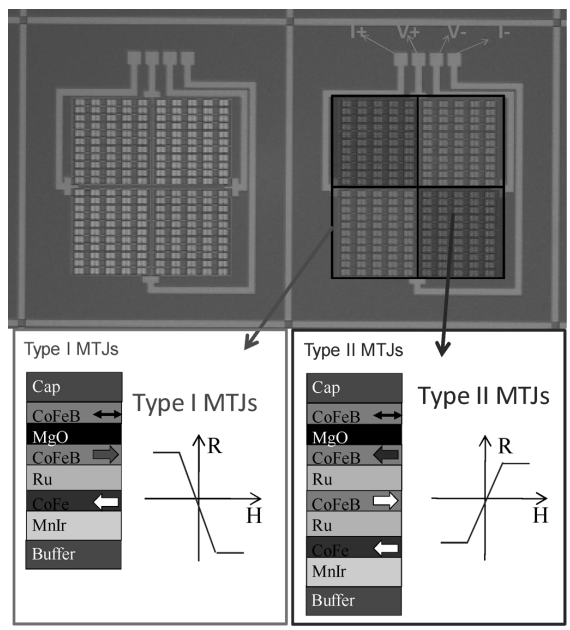

Fig. 4. Top: Optical microscope picture of Wheatstone Bridges. In order to maximize the Bridge output, two types of sensors, with symmetric output, are used. Bottom: MTJ stacks used in each arm of the bridge to provide the symmetric output required to obtain a full bridge signal.

was then patterned into 110 individual MTJs with $5 \times 70\ \mu\mathrm{m}^2$ connected in series and making up the different branches of a Full Wheatstone Bridge. The microfabrication process is summarized in Fig. 3.

A top view picture of the devices can be seen in Fig. 4. The regions occupied by the two different types of stacks are highlighted on the right hand side device.

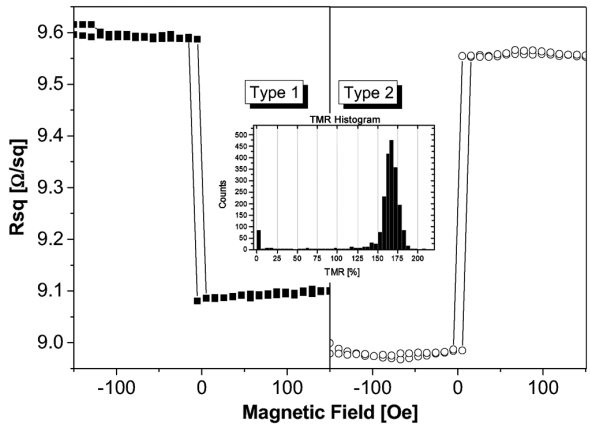

Fig. 5. CIPT transfer curve obtained from direct measurements in the stacks of Type 1 and Type 2 at the wafer surface before microfabrication of the Wheatstone Bridges. Inset: TMR histogram obtained from patterned isolated MTJ pillars fabricated in separate test wafers.

As shown in Fig. 4, after a common annealing step the orientation of magnetization in the CoFe layer adjacent to the anti-ferromagnet is the same in both stacks. However, due to the additional layers in the SAF of stack Type 2, the magnetization direction in the CoFeB adjacent to the MgO barrier points in opposite directions. With the reference magnetization direction in opposite directions, dR/dH should be symmetric in MTJs of the two stacks, as required for a Full Wheatstone Bridge. This method of producing MTJs with symmetric dR/dH values is compatible with large scale production of Wheatstone Bridges based in MTJ devices.

The two different orientations of the reference layer in the two stacks deposited was confirmed performing a bulk CIP transfer curve measurement, as shown in Fig. 5.

As expected, the low and high resistance states for each of the stacks are obtained with magnetic fields of opposite signal. The CIPT measurement also shows that the resistance values in the two MTJ stacks are not exactly the same. In fact, the RxA values obtained from CIPT are 10.7 $\mathrm{k}\Omega\mu\mathrm{m}^2$ and 11.5 $\mathrm{k}\Omega\mu\mathrm{m}^2$ for stacks of Type 1 and Type 2, respectively. This RxA imbalance between the two MTJ types should result in a bridge offset of 3.4%, apart from further lithographic area definition error during the microfabrication process. This RxA imbalance could be compensated with an asymmetry in the MTJ area targeting the production of bridge elements with the same final resistance. However this was not done since the accuracy of the CIPT measurement is not fully determined and a 3.4% offset is still considered reasonable.

The TMR value extracted from CIPT measurements is 174%, in good agreement with transport measurements performed in isolated patterned pillars in test wafers with similar stacks (inset of Fig. 5).

Upon successfully achieving the deposition of MTJ stacks with opposite dR/dH on the same wafer, the stacks were patterned into individual MTJs with an area of $5 \times 70\ \mu\mathrm{m}^2$ and the MTJs were interconnected, forming the full bridges with 110 MTJs connected in series in each bridge arm (Fig. 4).

The area of the MTJs was optimized to provide a good linear response with a short linear range (high sensitivity). Notice that

TABLE I
VSM CHARACTERIZATION OF THE FREE LAYER COMPONENTS

Material	Thickness	Magnetization
$Co_{40}Fe_{40}B_{20}$	3.0 nm	1359 emu/cm^3
$Ni_{81}Fe_{19}$	16.0 nm	788 emu/cm^3

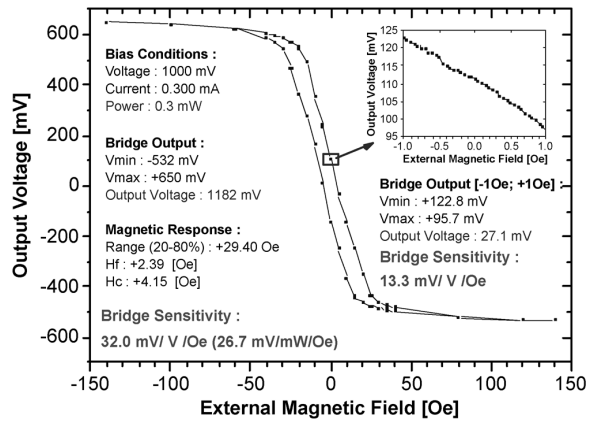

Fig. 6. Bridge Magnetometer output under a magnetic field sweep along reference layer magnetization direction. Inset: bridge ouput under a 1 Oe field sweep.

the 5 $\mu\mathrm{m}^2$ used for the width of each MTJ sensor are relatively large. This is a consequence of the enhancement of the demagnetizing field due to the thick NiFe in the free layer. The VSM measurements of the stacks represented in Fig. 3 allow the determination of magnetization of the NiFe and CoFeB in the free layer (Table I). Considering the measured magnetization and the relative thicknesses of the two layers, the introduction of NiFe should increase the magnetic moment of the free layer by a factor of 4.

The reason to use MTJs connected in series at each arm of the bridge is twofold: i) the bridge is able to endure a larger bias voltage, thus resulting in higher output signal and lower power consumption and ii) the magnetic field detection limit of N elements connected in series decreases with $\mathrm{N}^{0.5}$ [11]. The first reason is important from an application point of view. The ability to endure large input voltages is a requirement for applications targeting the automobile industry and low power consumption is particularly important for magnetometers operating within portable devices such as cellular phones. With 110 elements connected in series, the bridge should be able to endure more than 100 volts without the breakdown of the tunnel barriers. Furthermore, the bridge voltage output increases proportionally to the bias voltage thus reducing the amplification requirements for any associated electronic readout circuit.

III. ELECTRICAL CHARACTERIZATION

Upon micro fabrication the bridge performance was evaluated by monitoring the output of the bridge under a variable intensity magnetic field sweep with the external magnetic field directed along the reference layer magnetization direction (coincident with the MTJ short axis). The result can be seen in Fig. 6.

Sweeping the field between -140 Oe and $+140$ Oe, the bridge exhibits a linear response along a range of about 29 Oe (corresponding to voltage a variation between 20% and 80% of the total voltage excursion). While this short range provides

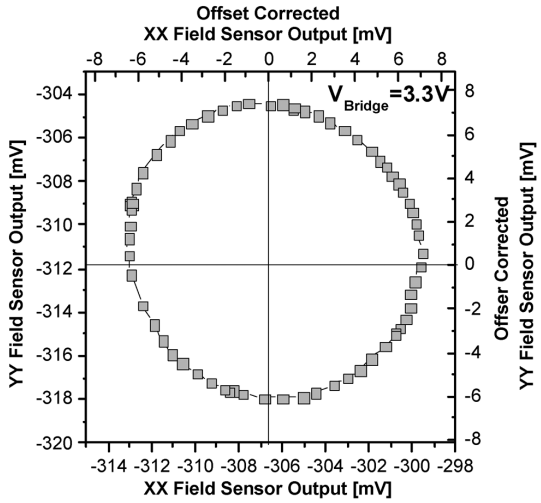

Fig. 7. 2-axis MTJ Full Bridge Magnetometer output measured in a digital compass electronic reading unit during a 360 degree rotation.

good sensitivity, the effective coercivity of the bridge is still relatively large (4.15 Oe). This effective coercivity results from the combined contributions of the sensing layer coercive field, stray fields and demagnetizing field upon pillar micro fabrication and variations in the individual MTJ response making up the MTJ series. Despite the effective coercivity value, a small loop sweep still displays reversible characteristics.

The offset of the bridge is of the order of 10% of the total output which large compared to the 3.4% estimate obtained from the CIPT RxA measurements. Both additional lithographic area definition errors and the effective coercivity contribute to this result.

When biased with 1 V the bridge output changes between $+650$ mV and -532 mV (total voltage excursion is 1182 mV) under a large magnitude field sweep. From these values, a bridge sensitivity of 32 mV/V/Oe (26.7 mV/mW/Oe) is obtained. Typical commercial products integrating AMR devices in bridge configuration exhibit sensitivities of 1 mV/V/Oe. However, when a small magnitude field sweep is applied the resulting voltage variation is not in the same proportion.

For a field sweep between -1 Oe and $+1$ Oe the total voltage variation obtained is 27.1 mV under the same 1 V bridge bias. This means that the bridge sensitivity calculated with this small field sweep is now only 13.3 mV/V/Oe. While this is still a large value compared with the existing commercial products, it is smaller than what would be expected if the linearity of the sensor was perfect. This is a point which can still be improved with the introduction of weakly pinned free layers [12].

In order to demonstrate the feasibility of MTJ Full Wheatstone bridge magnetometers, a 2-axis magnetometer was constructed by joining in the same chip two bridges mounted with reference directions oriented at 90 degrees of each other. This chip was integrated in a digital compass platform. Fig. 7 shows the output of the two magnetometers measured in the platform during a 360 degrees rotation. The output is non-hysteretic and the departure from an ideal circle is attributed to placement error of the bridges in the chip carrier.

The total output of the magnetometers for each axis is 13.5 mV, a value large enough to be measured without any type of signal amplification. Using the bridge sensitivity measured for small fields (13.3 mV/V/Oe) and considering the bias voltage of 3.3 V used in the electronic platform, the field intensity can be quantified. A value of 0.31 Oe is obtained, which is consistent with the magnitude expected for the geo-magnetic field.

IV. Conclusions

Full Wheatstone Bridges were produced using full signal CoFeB/MgO/CoFeB magnetic tunnel junctions. The resulting bridges exhibit sensitivities of the order of 13.3–32.0 mV/V/Oe depending on the field range considered. A 2-axis magnetic field magnetometer was constructed using the MTJ bridges and effectively used as compass unit detecting the earth's magnetic field.

Acknowledgment

This work was supported by the European project SE2A—Security and Energy Efficient Systems for Automotive Industry.

References

[1] M. D. Cubells-Beltrán, C. Reig, D. Ramírez, S. Cardoso, and P. P. Freitas, *IEEE Sens. J.*, vol. 9, pp. 1756–1762, 2009.
[2] S. Ikeda, J. Hayakawa, Y. Ashizawa, Y. M. Lee, K. Miura, H. Hasegawa, M. Tsunoda, F. Matsukura, and H. Ohno, *Appl. Phys. Lett.*, vol. 93, p. 082508, 2008.
[3] G. Malinowski, M. Hehna, F. Montaignea, A. Schuhla, C. Duretb, R. Nantuab, and G. Chaumontet, *Sens. Actuators A*, vol. 144, pp. 263–266, 2008.
[4] J. M. Teixeira, J. Ventura, M. P. Fernandez-Garcia, J. P. Araujo, J. B. Sousa, P. Wisniowski, D. C. Leitao, and P. P. Freitas, *J. Appl. Phys.*, vol. 111, p. 053930, 2012.
[5] S. Ikeda, K. Miura, H. Yamamoto, K. Mizunuma, H. D. Gan, M. Endo, S. Kanai, J. Hayakawa, F. Matsukura, and H. Ohno, *Nature Materials*, vol. 9, pp. 721–724, 2010.
[6] J. M. Almeida and P. P. Freitas, *J. Appl. Phys.*, vol. 105, p. 07E722, 2009.
[7] Y. Jang, C. Nam, J. Y. Kim, B. K. Choa, Y. J. Cho, and T. W. Kim, *Appl. Phys. Lett.*, vol. 89, p. 163119, 2006.
[8] W. Shen, B. D. Schrag, A. Girdhar, M. J. Carter, H. Sang, and G. Xiao, *Phys. Rev. B*, vol. 79, p. 014418, 2009.
[9] P. Wiśniowski, J. M. Almeida, S. Cardoso, N. P. Barradas, and P. P. Freitas, *J. Appl. Phys.*, vol. 103, p. 07A910, 2008.
[10] J. Cao and P. P. Freitas, *J. Appl. Phys.*, vol. 107, p. 09E712, 2010.
[11] R. J. Janeiro, L. Gameiro, A. Lopes, S. Cardoso, R. Ferreira, E. Paz, and P. P. Freitas, "Linearization and field detectivity in magnetic tunnel junction sensors connected in series incorporating 16 nm-thick NiFe free layers," *IEEE Trans. Magn.*, submitted for publication.
[12] R. Ferreira, E. Paz, P. P. Freitas, J. Wang, and S. Xue, "Large area and low aspect ratio linear magnetic tunnel junctions with a soft-pinned sensing layer," *IEEE Trans. Magn*, submitted for publication.